MEASUREMENT OF ENERGY ABSORPTION IN

OMNIDIRECTIONAL PHOTON FLUXES

Fearghus O'Foghludha

Department of Radiology, Medical College of Virginia
Richmond, Virginia

Emanuel Rind

NASA Langley Research Center
Langley Station, Hampton, Virginia

Presented at the Virginia Academy of Science

MEASUREMENT OF ENERGY ABSORPTION IN

OMNIDIRECTIONAL PHOTON FLUXES

Fearghus O'Foghludha

Department of Radiology, Medical College of Virginia

Richmond, Virginia

Emanuel Rind

NASA Langley Research Center

Langley Station, Hampton, Virginia

ABSTRACT

A quick and versatile technique has been experimentally developed for measuring average dose from spatially distributed gamma radiation in a mass system, i.e., a body organ or the body itself. The technique and resulting data within statistical error are in agreement with King's reciprocity theorem. Experimental data also show that although the theorem ignores photon scattering, it is still valid. The technique is being extended to neutron produced doses. The experimental equipment is described and experimental results are presented.

MEASUREMENT OF ENERGY ABSORPTION IN
OMNIDIRECTIONAL PHOTON FLUXES

Fearghus O'Foghludha

Department of Radiology, Medical College of Virginia

Richmond, Virginia

Emanuel Rind

NASA Langley Research Center

Langley Station, Hampton, Virginia

SYMBOLS

D_{av} average absorbed dose per unit mass

D distributed absorbed dose in the differential mass

M mass

dm differential mass

Σ total energy (dose) deposition in a mass (M)

R dose exposure rate at source position

Cr-51   chromium isotope, atomic mass No. 51

Zn-65   zinc isotope, atomic mass No. 65

MeV   million electron volts of energy

E gamma energy

$N(E)$ distribution function for the gammas as a function of their energy

k constant of proportionality

In^{113m} indium isotope, atomic mass No. 113, metastable

Sn^{113} tin isotope, atomic mass No. 113

Au^{198} gold isotope, atomic mass No. 198

Co^{60} cobalt isotope, atomic mass No. 60

INTRODUCTION

Basic Problem

Charged particles hitting the walls of a spacecraft produce bremsstrahlung, characteristic X-rays, and de-excitation gammas which can bathe an astronaut in an omnidirectional photon flux (fig. 1). The photon flux is not necessarily isotropic and is far more penetrating than the bombarding particles that give rise to it. Although the resulting dose is small in comparison with that derived from protons in space (with the exception of those in the Van Allen electron belts where it has been estimated at some rads/hour[1]), it is not negligible, and should be accurately measured. Adequate specification of the dose involves, ideally, a complete knowledge of the spatial distribution. Since this is difficult to determine, a statement of the more easily comprehended average dose D_{av} would appear at first sight to be an acceptable alternative. Finding D_{av}, however, itself involves integration over the volume throughout which the dose varies and subsequent division by the total mass

$$D_{av} = \int_M D dm \bigg/ \int_M dm \qquad (1)$$

so that even if one is content with the average dose, evaluation of the numerator in the above expression - which amounts to knowing the spatial distribution - is again unavoidable. Chemical measurement methods, which automatically perform the integration, yield D_{av} directly; but, in order to mock-up suitable incident fluxes for such determinations, sources which are capable not only of reproducing the desired flux pattern but are also of sufficient intensity to actuate the dosimeter solutions are required. This in practice makes average dose measurement both expensive and hazardous.

Reciprocity Principle

In a search for an easier method for determining the average dose, we have used the so-called radiation reciprocity theorem, first stated by King almost 60 years ago[2]. The principle states (see fig. 2) that the total energy deposition, i.e., the quantity

$$\Sigma = \int_M Ddm \qquad\qquad (2)$$

in an absorber exposed to an external source is proportional to the exposure rate R which would be observed at the source position if the body were a radiator; because D_{av} is, from expressions (1) and (2) equal to Σ/M, it follows that D_{av} and R are also proportional. King's reciprocity relation holds because, as shown in figure 2, Σ and R are given by two integrals which differ from each other in constants only. King's derivation neglects photon scattering, which might limit the principle severely in practical cases where Compton collisions are often the main energy-transfer mechanism. Our first task was to demonstrate experimentally that scattering does not appreciably alter the validity of the theorem, and this we have done[3] by a method which need not concern us now. Figure 3 illustrates, as an example, the way in which Σ (dots) and R (crosses) depend on body thickness at an energy of about 0.5 MeV. It is seen that R and Σ remain proportional over the range of thicknesses used, so that a measurement of R also gives us a quantity proportional to Σ and hence to the average dose D_{av}. We might have anticipated that scattering would affect matters little by examining figure 4; it seems plausible to assume that the effects of radiation which in arrangement (a) can reach a point P only if there is scattering, will be compensated for in the inverse or conjugate case (b) by radiation from P which, similarly, can reach

the detector only if scattering occurs. However, the agreement represented by figure 3 is rather better than might have been expected, because the suggested cancellation process cannot be exact; this follows because multisegment photon paths are not reversible, since the energy (and hence the interaction probability) depend on the order in which the segments are traversed. Whatever the theoretical basis, it is nevertheless experimentally known that Σ/E is constant within acceptable limits for tissue-like absorbers in the range of photon energies of interest to us.

Practical Application

In applying the principle to our problem, we do this: an astronaut exposed to an omnidirectional flux can be considered to be exposed to an array of sources arranged in a suitable pattern over the surface of a sphere, or exposed to one such source which is moved over the surface in an appropriate way, as suggested in figure 5. According to the reciprocity principle Σ (or D_{av}) may be calculated from the readings of multiple dosimeters arranged around a radioactive analog of the astronaut or by integrating the readings of a single instrument moving over the sphere surface in the correct pattern. If we wish to measure Σ or D_{av} in a single organ rather than in the whole body, we fill the organ of interest with radioactive material, leaving the surrounding body inactive.

Flux Anisotropy

The technique can also be applied in the study of anisotropic bombarding fluxes. Our interest in such patterns arises because, if the flux is nonuniform, the whole-body or single-organ average dose may be sensitive to astronaut attitude. The occupant of an earth-orbiting craft might, for example, be

better off as far as gonad dosage is concerned if he flew with his head towards the earth. In a polar orbit, it is possible that his dose would depend on whether he lay along the magnetic field lines or at right angles to them. Even in a uniform particle flux there might be certain pilot orientations within an asymmetric craft along which the average dose would be smallest, since the photon fluxes emerging from various parts of the walls would be different.

The effects of anisotropy can be investigated, whether we use multiple stationary detectors or a single movable one, by weighting the readings according to the fluxes expected to arrive from the various directions. With the multiple-detector system, however, we can also take into account the motion of the astronaut with respect to some fixed feature of the flux pattern, by making him move during the observations. For various reasons we have used only one detector in our work. This, of course, allows all the same investigations to be made, but at much greater labor than if multiple detectors were employed. A further complication is that in our experiments space limitations make it difficult to drive a shielded detector over a spherical surface so that we are forced to hold the detector stationary and move the phantom in the correct pattern of relative motion.

DESCRIPTION OF EXPERIMENTAL PROCEDURE AND SETUP

The phantom we use is a fully compartmented "Remcal"[*] without skeleton. It sits in a chair (fig. 6) which can be driven continuously about three mutually perpendicular axes. Because balancing is important if the driving motors are not to experience variable loads during a motion cycle, the phantom is strapped into a moulded fiber-glass shell. To permit investigation of

---

[*]Alderson Research Laboratories, 48-14 33rd Street, Long Island City, N.Y.

nonuniform fields, the driving motors are speed-programed so that the phantom moves slowly when it is oriented in a direction from which the incident flux is expected to be large and quickly in orientations of low-incident intensity. About the pitch and roll axes, the programing is done by means of a curve follower. This has the inherent disadvantage that errors are cumulative, since the speed impressed at any one instant is calculated on the assumption that the carriage has correctly followed all previous instructions. This assumption may be in error due to the high carriage inertia. About the azimuthal axis, where inertial problems are greatest, we have had to rely on a simple cam-follower system in which cumulative errors do not occur. Figure 7 shows the motor controls, servoposition indicator, TV system, and a multichannel analyzer whose purpose will be described shortly.

The phantom is filled with dilute solutions (about 10 microcuries per liter) of various monoenergetic gamma emitters ranging from Cr-51 (0.32 MeV) to Zn-65 (1.12 MeV). We introduce the solutions by using a peristaltic pump or, more safely, by topping up the filled inactive phantom with very small volumes of high specific activity material. Monoenergetic sources alone cannot, of course, directly simulate the continuous bremsstrahlung spectrum liberated in the capsule walls. However, by performing the experiments with a variety of monoenergetic emitters, we can synthesize the response which would have been obtained if the individual components were combined in amounts appropriate to the continuous spectrum that is being simulated.

Detectors

The principal advantage of the reciprocity technique, that is, the use of cheap, low-intensity emitters, disappears if the external detectors are insensitive. Our first detectors were miniature Geiger brain probes which, in spite

6

of their energy dependence, are satisfactory in radiation spectra of the type

we have encountered[4], but we soon replaced them with scintillation detectors.

Sodium iodide is unusable in this application (unless the signal is processed

in a complex way[5]) because of the extreme energy dependence, but low-Z phos-

phors such as anthracene and various solid solutions of p-terphenyl derivatives

are perfectly acceptable[6]. Our first scintillation instrument (fig. 8) used

a cylindrical anthracene crystal 1/2-inch by 1/2-inch diameter, coupled by

means of a lucite light guide to a photomultiplier with a 1-inch-diameter

cathode. The total light output was measured with a sensitive electrometer

and was shown, in separate experiments for both anthracene and the plastic

phosphor, NE 102, to be independent of the quantum energy within acceptable

limits. (See fig. 9.) Electrometric measurements are uncertain and have now

been replaced by pulse counting, in which the area under the pulse-height spec-

trum, suitably weighted to take account of the energy deposition per pulse, is

taken as a measure of the energy deposition in the phosphor and hence of the

exposure in its vicinity. The method, of course, gives the same answer as mea-

suring the total current but eliminates the drift of electrometer techniques

and permits us to integrate over lengthy periods, which is not easy when we rely

on the total current. The result of the weighting process is represented by the

integral

$$\int_0^{E_{max}} E \cdot N(E)dE$$

where $N(E)dE$ is the number of gammas having energies in the interval $(E + \Delta E)$.

The integral was first evaluated manually but the process is now carried out

automatically by counting the number of pulses delivered during the period of

observation by the 8 Mc/s clock generator in the analog-to-digital converter of

the pulse-height analyzer. Since the clock circuit delivers a number of pulses proportional to E, say kE, for each pulse corresponding to energy E and delivers nkE pulses for n such pulses, it is clear, by extension to all energies, that the output of the generator gives the desired integral directly.

In the interest of sensitivity, the NE 102 detector has been increased in size to 3 inches by 3 inches, as shown on the right-hand side of figure 10. In order to determine the energy dependence, which, at least for small phosphor sizes, is negligible, we have had to use the current method since fluxes low enough not to saturate the electronics cannot ordinarily be measured with ionization chambers with calibration traceable to a standardizing laboratory such as the National Bureau of Standards. A difficulty in working with the spectra generated in organic materials is that there are no prominent features - since the photoelectric cross section is small - and energy calibration by admission of (monoenergetic) conversion electrons through a window in the phosphor housing is necessary.

Despite the relatively small energy dependence, it is still necessary to know the extreme of spectral distortion. Our experiments on this point have absorbed by far the greatest part of our energies in this entire project[4]. Spectral distortion arises because the photons, even though monoenergetic at emission, are degraded in energy by scattering as they push their way outwards towards the detector. Although the presence of these scattered photons is easily demonstrated by examination of scintillation pulse-height spectra, the intensity cannot be found without further processing of the spectra. Thus in figure 11, which compares the pulse-height spectrum of a 25-cm-thick water layer containing Zn^{65} with that of a point source of Zn^{65} in scatter-free conditions, we see that in the extended-source case a given number of full-energy

8

pulses is accompanied by a larger number of low-energy events than if scatter-free conditions obtain. For convenience of comparison, the spectra have here been normalized to equal photopeak counts. We cannot assume, however, that the photon intensities at a given energy are in the ratio of the pulse frequencies at the corresponding pulse heights. In fact, because the pulse-height spectra are a reflection only of the distribution-in-energy of the secondary electron liberated in the detector material, we know little of the photon (or "time") spectra themselves. To get this information we must "unscramble" the pulse-height spectra by means of the well-known matrix inversion technique (7) which removes instrumental distortions and reveals the original photon spectra. When this technique is applied to the pulse distributions of figure 11, the photon spectra of figure 12 are obtained. The relative amount of scattered radiation accompanying the primary Zn^{65} photons (energy 1.12 MeV) is now seen to be much less than inspection of figure 11 would suggest. In fact it is easy to show that the plastic phosphor detectors we are using (8) can deal adequately with scattered photon spectra similar to that represented by the shaded histogram of figure 12, and are negligibly affected by changes in spectral distribution as the phantom changes its orientation with respect to the detector.

DISCUSSION OF RESULTS

Dependence of D_{av} on Body Orientation

Some results on the variation of average dose with body orientation are shown for an energy of 0.39 MeV in figure 13. The gamma rays are derived from In^{113m}, a very suitable material for these experiments because of its short half-life (1.7 hours) which reduces contamination problems, and because of its easy availability as a daughter product of Sn^{113} (half-life 118 days).

Curves marked with circles show the way in which the average whole-body (phantom) dose varies with zenith angle. The zenith angle is defined as the angle the photon trajectory makes with respect to the horizontal plane of the body and is measured from 0° to 360°. When the radiation approaches downwards through the head (90° zenith angle) or upwards through the feet (270° zenith angle), the energy deposition is, as we expect, smaller than when the photon approach is made from angles intermediate to these two; but the difference is much less spectacular than if the projected surface area of the body (9), as shown by the dashed curve, were the only factor operating. In fact, when the body meets the photons head on (90° zenith angle), reduction in impact area is partially compensated by the greater tissue thickness backing this smaller area, and so the chance of total absorption is increased. This effect presumably depends on whether the body or phantom is sitting or standing; but, because the fiber-glass support shell is designed for the sitting position, we have not yet been able to investigate this. Too, at present, there are insufficient measurements at enough energies to deduce with confidence the results obtained with an incident photon continuum.

Figure 13 also shows results for the liver, where the variation is quite pronounced. In both cases illustrated, the incident flux is uniform. When the flux depends on $\cos^2\theta$ where θ is the zenith angle, we find that the average whole-body dose varies by only some 10 percent when the orientation of the body axis to the direction of the flux path changes from 0° to 90°. The liver dose on the other hand is 50 percent less when the body leads head on into the direction of the flux path than if it leads into it at 90° to the head-on position. The reduction is slightly different, about 45 percent, if it leads with its

feet. This is the kind of information we are now extracting for a large number

of possible flux patterns and for a variety of organs in the body.

CONCLUSIONS

The technique used for measuring photon dose is versatile and quick, but

has some drawbacks. These are: The limitation of suitable and available gamma

emitters for supplying a range of useful energies, although the scaling tech-

nique of Johansson[10] may overcome this difficulty. Contamination problems

arise if long-lived nuclides are used. We do not fully understand the effects

of scattered radiations from the walls of the room in which the experiments are

carried out, nor can we easily allow for the effects of the steel fork sup-

porting the phantom. Lastly, though this is unconnected with the validity, or

otherwise, of the reciprocity principle, we do not know what input bremsstrah-

lung spectra to use. Perhaps in these circumstances our scheme of working with

monoenergetic emitters is a fortunate one, since any continuous spectrum, as we

have seen, can be dealt with if the behavior of the individual components of

the continuum is understood. Although the method is theoretically applicable

to protons, whose interaction with the body is of great astronautical impor-

tance, suitable extended proton sources for use in the conjugate experiments

are not available and so the method fails in this case. There is a promising

application, however, in neutron studies $\left(\text{Bethe}[11]\right)$ and we have already begun

to investigate production of extended liquid neutron sources suitable for filling

the phantom, using soluble beryllium salts in aqueous solutions of α-emitting

substances.

Several incidental investigations have become necessary as parts of the

main program and are in progress. One is the use of Compton scattering as a

means of producing radiation of continuously variable energy. Availability of such radiation makes it possible to increase the effective number of input lines in the construction of response matrices for photon spectral studies. With the better response matrices obtained in this way, the notorious inaccuracy of the matrix inversion technique will be lessened. Finally, in order to obtain input data for our reciprocity measurements it will be necessary to carry out spectral measurements on electron-generated bremsstrahlung for various angles of electron incidence.

REFERENCES

1. Le Galley, D. P., and Rosen, A., in "Space Physics", p. 736, Wiley (New York), 1964.

2. King, L. V., Phil. Mag., 23, 242 (1912).

3. O'Foghludha, F., Phys. Med. Biol., 9, 155 (1964).

4. O'Foghludha, F., Phys. Med. Biol., 11 (1), 152 (1966) - Abstract.

5. Moriuchi, S., and Miyanaga, I., Health Phys., 12, 541 (1966).

6. Belcher, E. H. and Geilinger, J. E., Brit, J. Radiol., 30, 103 (1957).

7. Hubbell, J. H. and Scofield, N. E. Trans I.R.E. NS-5, 156 (1958).

8. O'Foghludha, F. NASA NGR 47-002-004, Status Report No. 2 (1966).

9. Guibert, A. and Taylor, C. L., USAF TR 7606, Wright-Patterson Air Force Base, Ohio, December 1951.

10. Johansson, S.A.E., Nucl. Sci. and Eng., 14, 196 (1962).

11. Bethe, H. A., Los Alamos Report 1428, June 20, 1952.
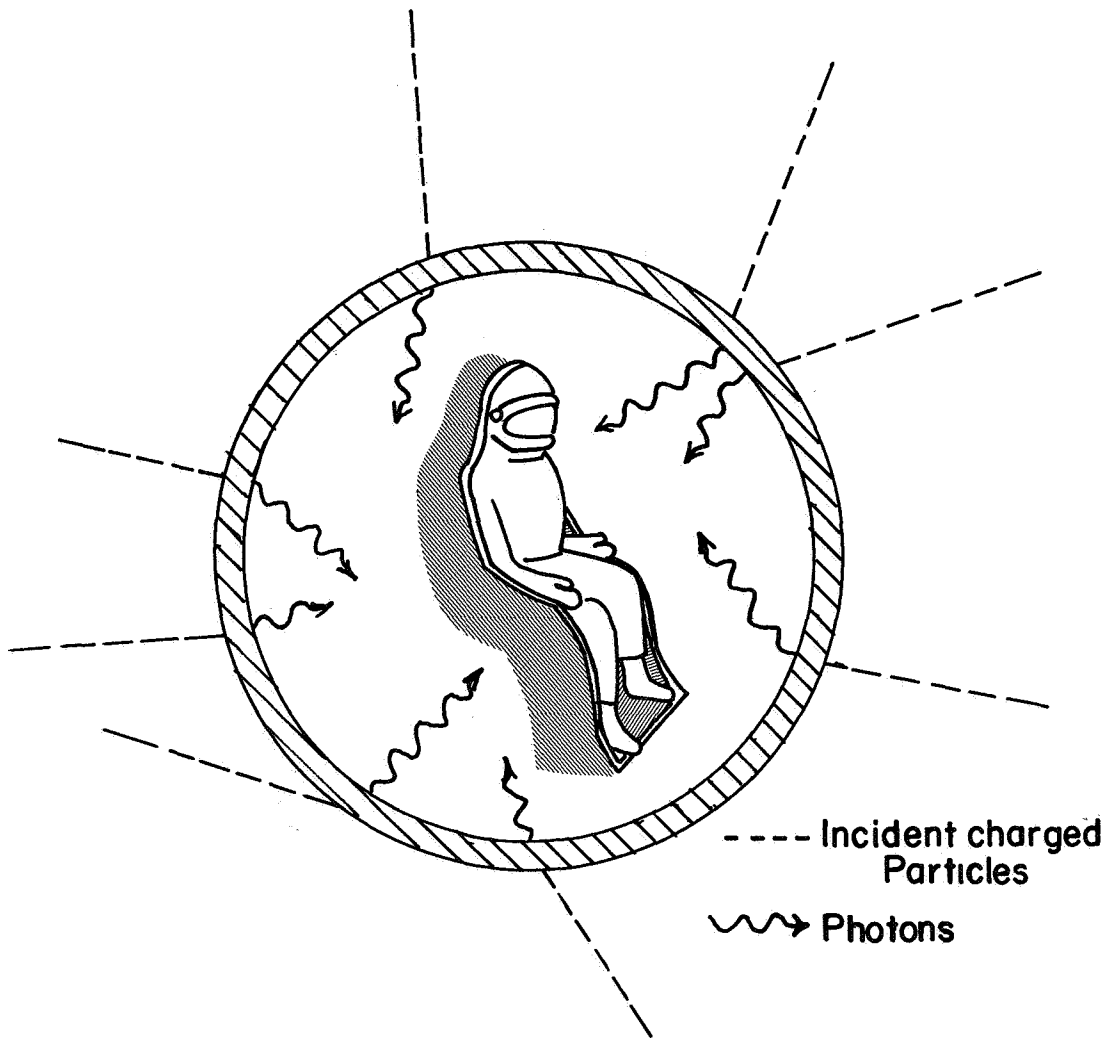
Figure 1.- Bremsstrahlung production in space vehicle walls.

(a)

$$\Sigma = \text{Const.} \int_V \frac{e^{-\mu z}}{(f+z)^2} \, dV$$

(b)

$$R = \text{Const.} \int_V \frac{e^{-\mu z}}{(f+z)^2} \, dV$$
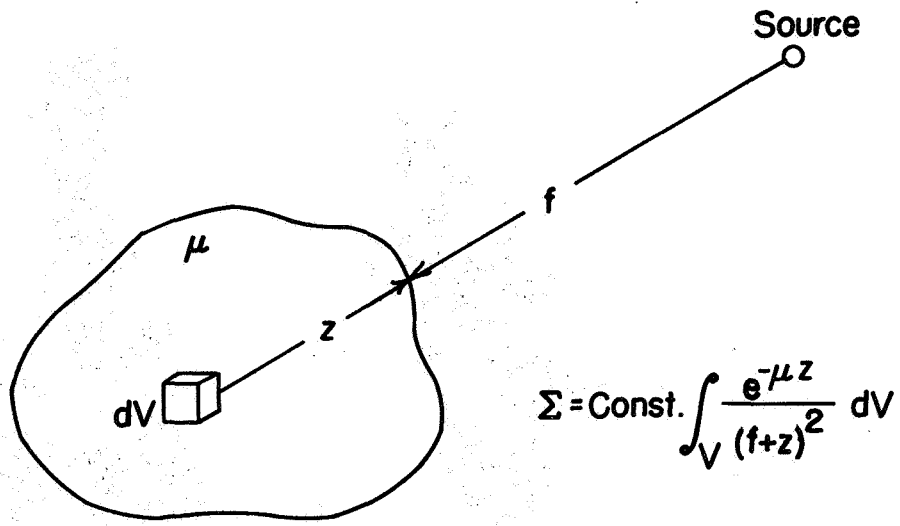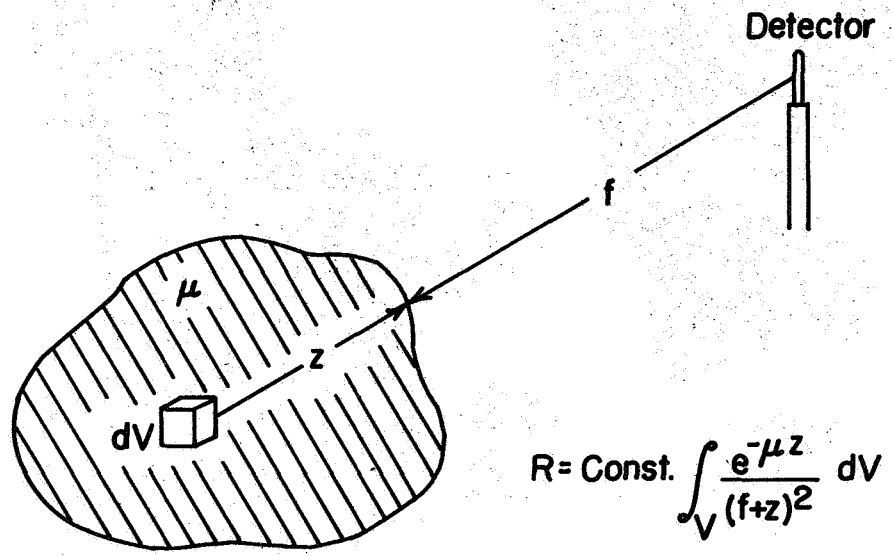
Figure 2.- Diagram illustrating the radiation Reciprocity theorem.
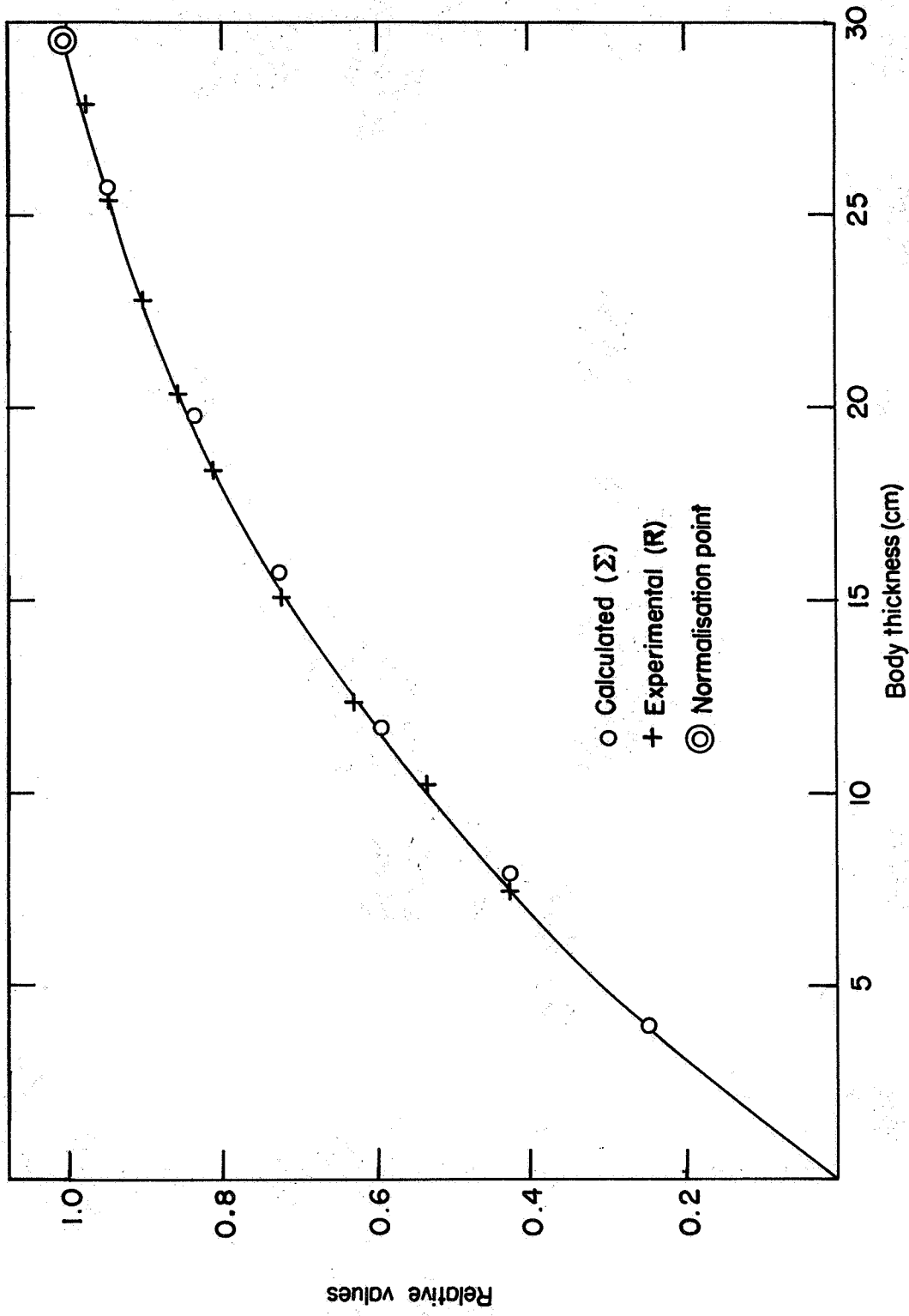
Figure 3.- Plot of total energy deposition (Σ) and dose exposure rate (R) at source position versus body thickness for $\sim$0.5 MeV gamma showing proportionality between Σ and R and dependence on body thickness.
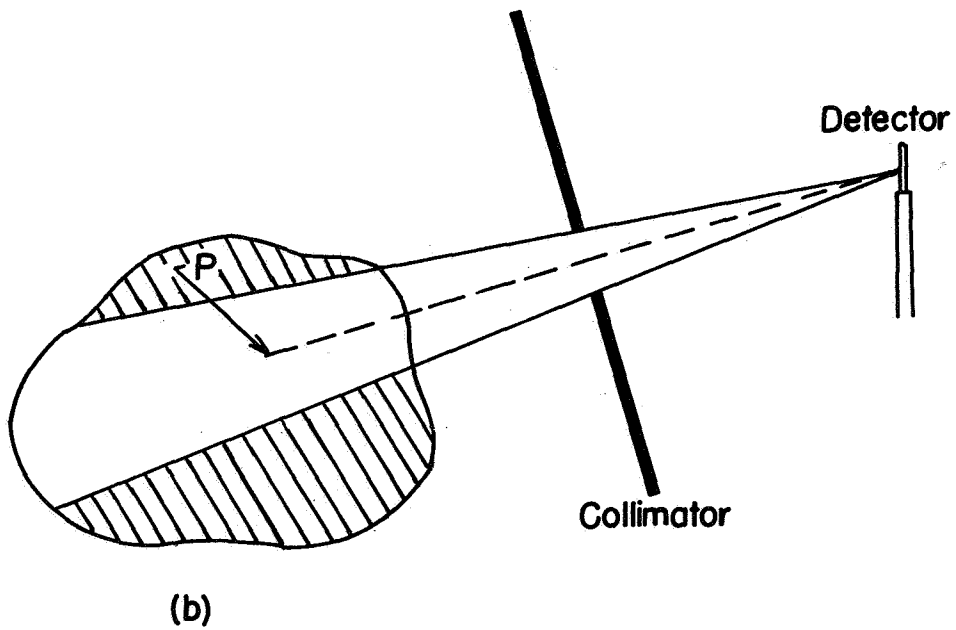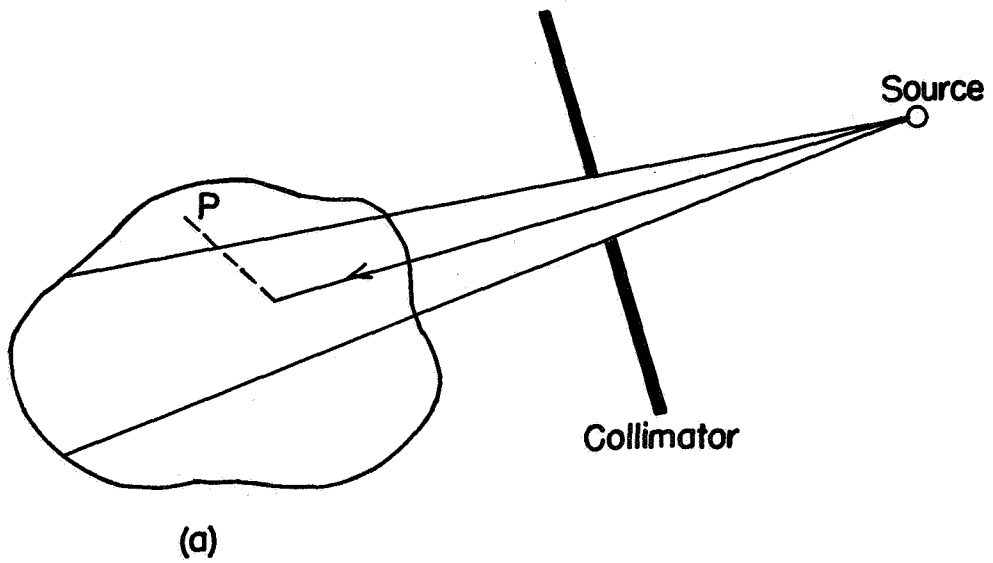
Figure 4.- Diagram illustrating the self-compensating effects of photon scattering on Σ and R which helps maintain their proportionality.
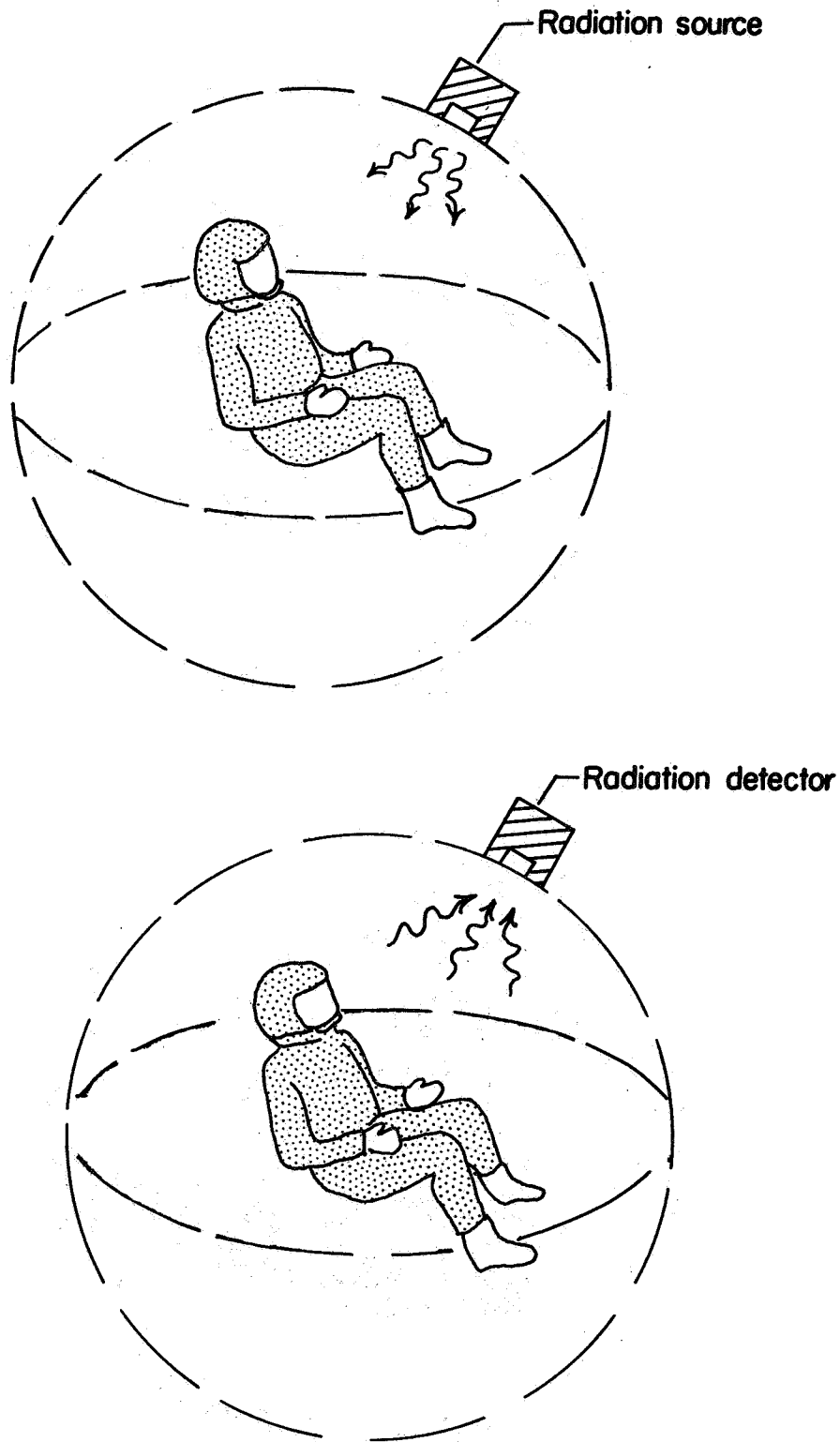
Figure 5.- Schematic drawing showing how omnidirectional or nonuniform gamma radiation is obtained and the reciprocity principle applied by having the source and detector traverse the same spherical path segments for given time intervals. This is done by driving the sphere while the source and detector remain stationary.
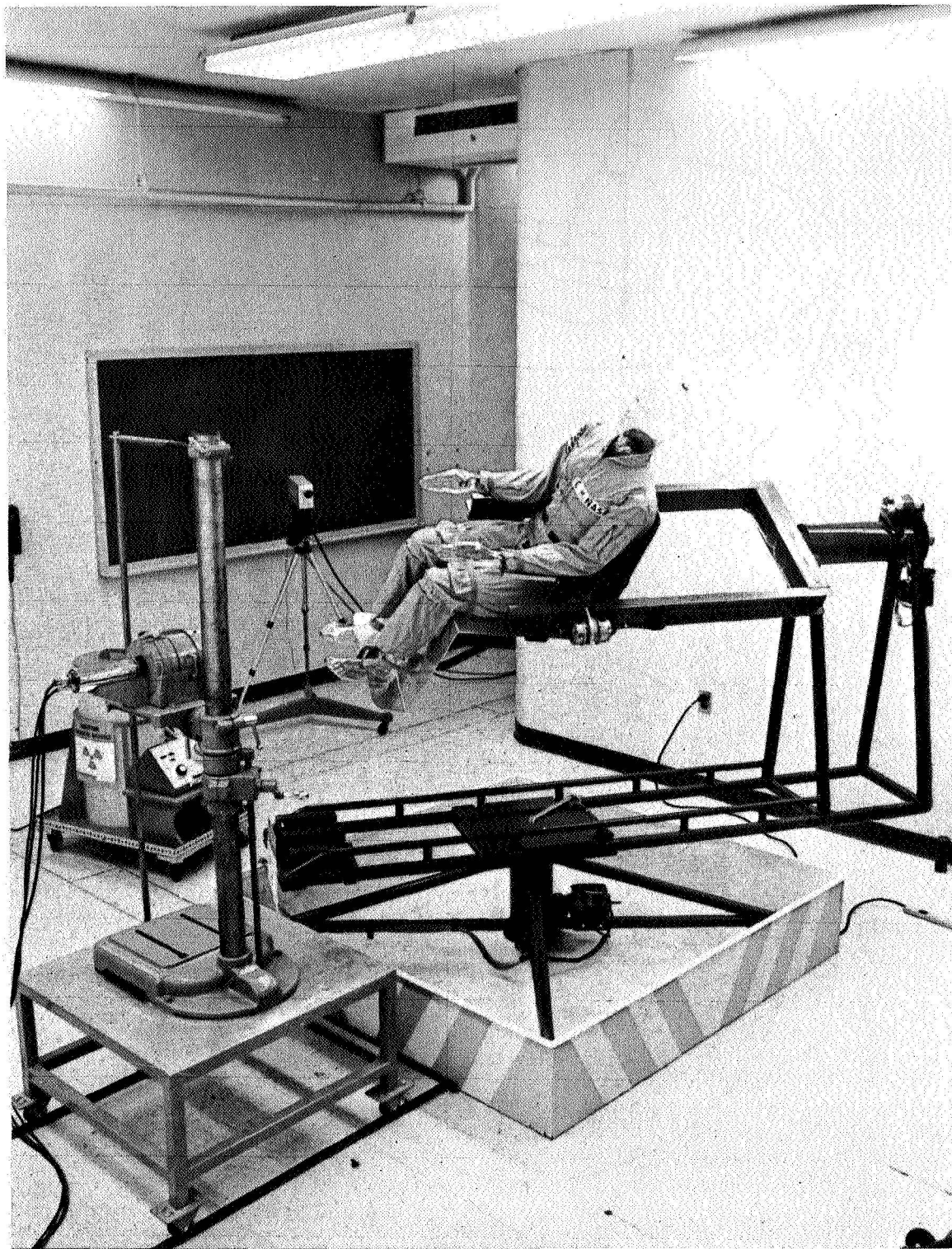
Figure 6.- Photograph showing phantom mounted on driving apparatus.
The moulded fiber-glass shell is not being used.
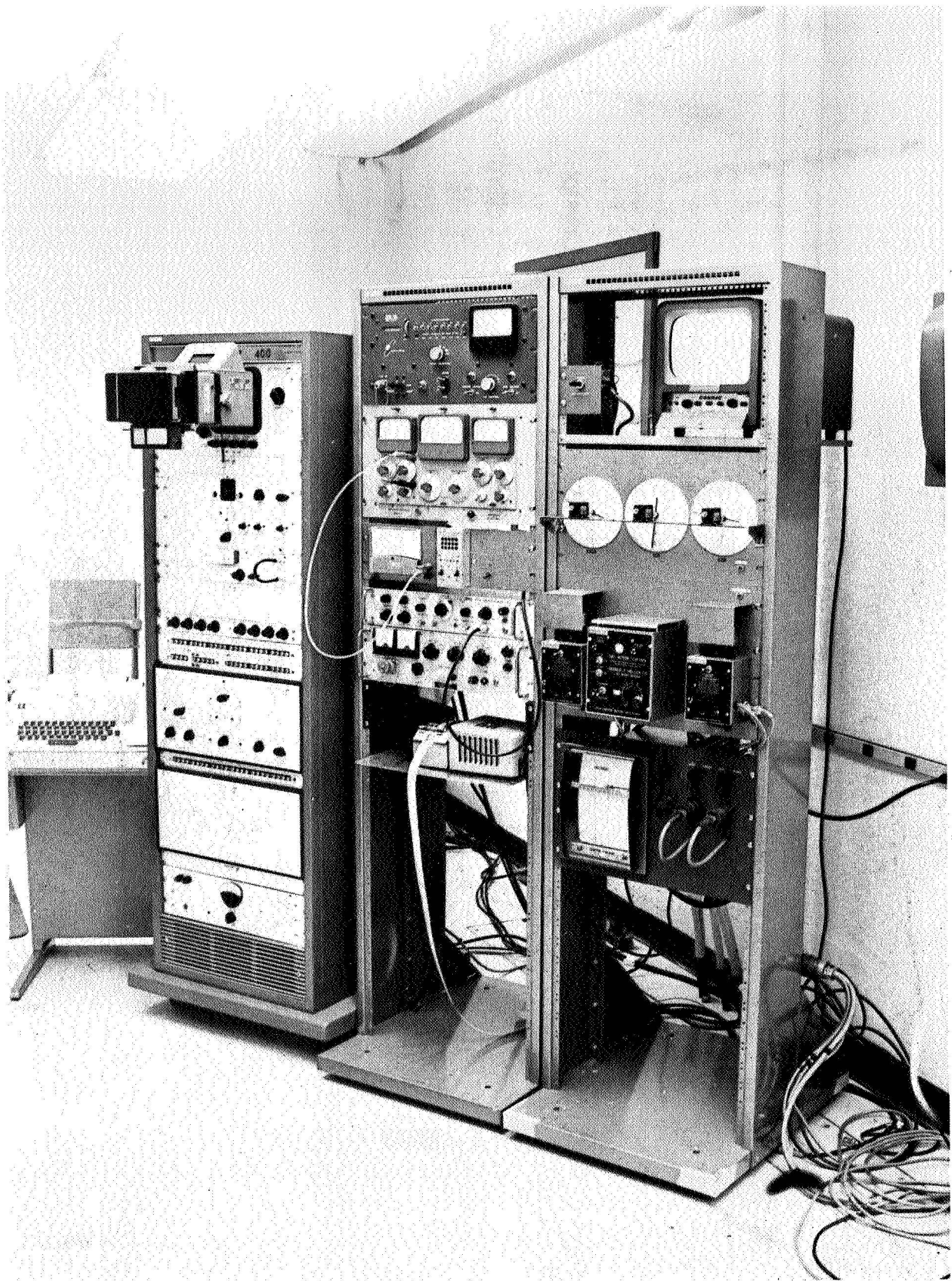
Figure 7.- Photograph showing motor controls, servoposition indicator,
TV monitoring, and pulse height analyzer system.
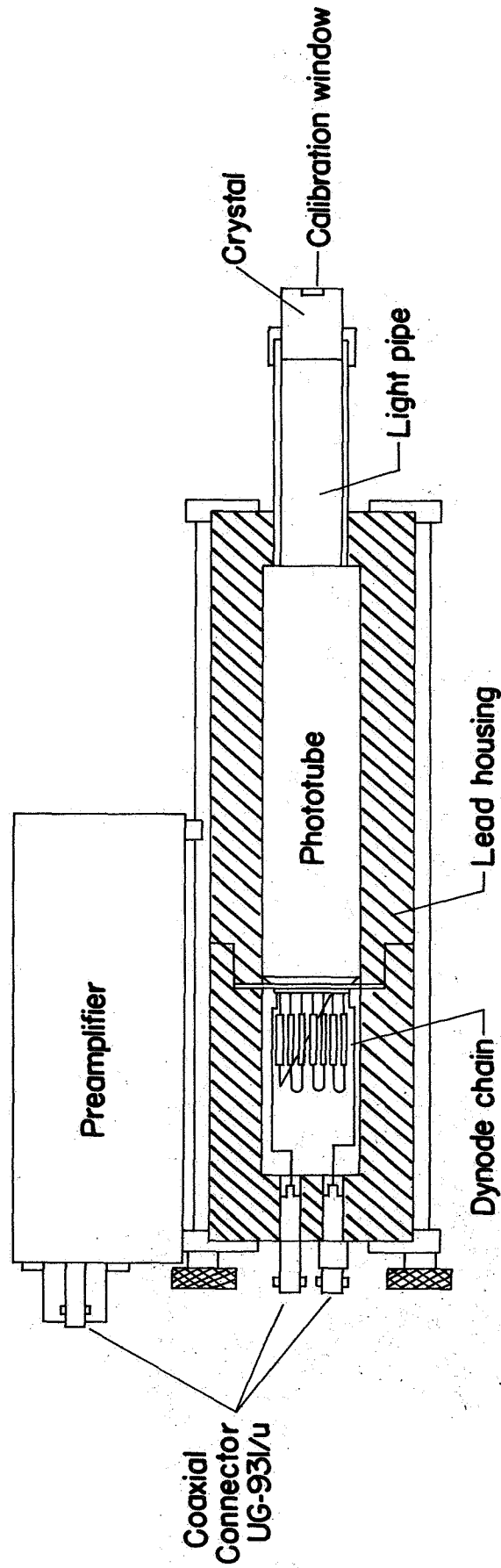
Figure 8.- Drawing of the anthracene scintillation detector.
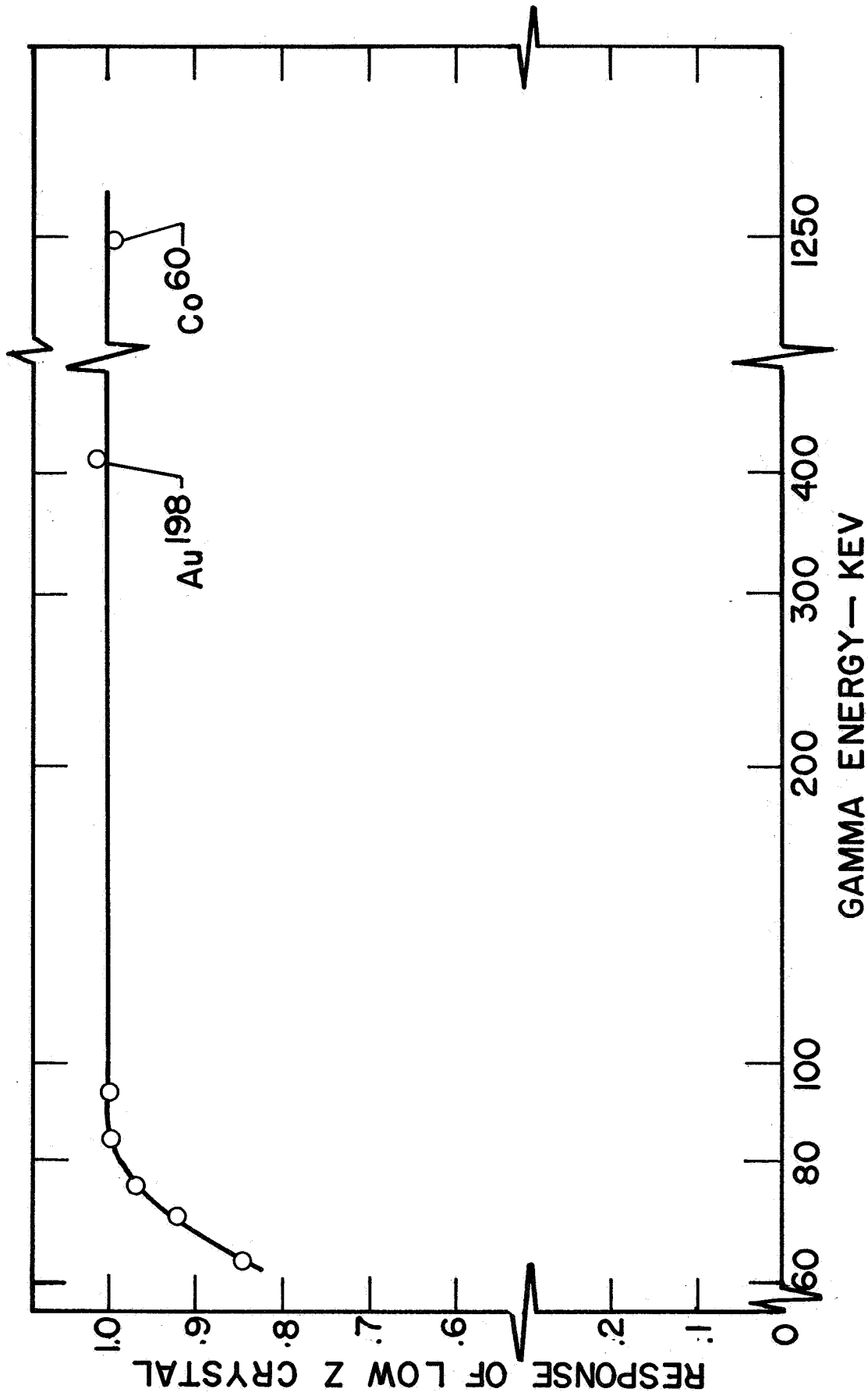
Figure 9.- Response of low atomic number phosphors versus gamma energy.
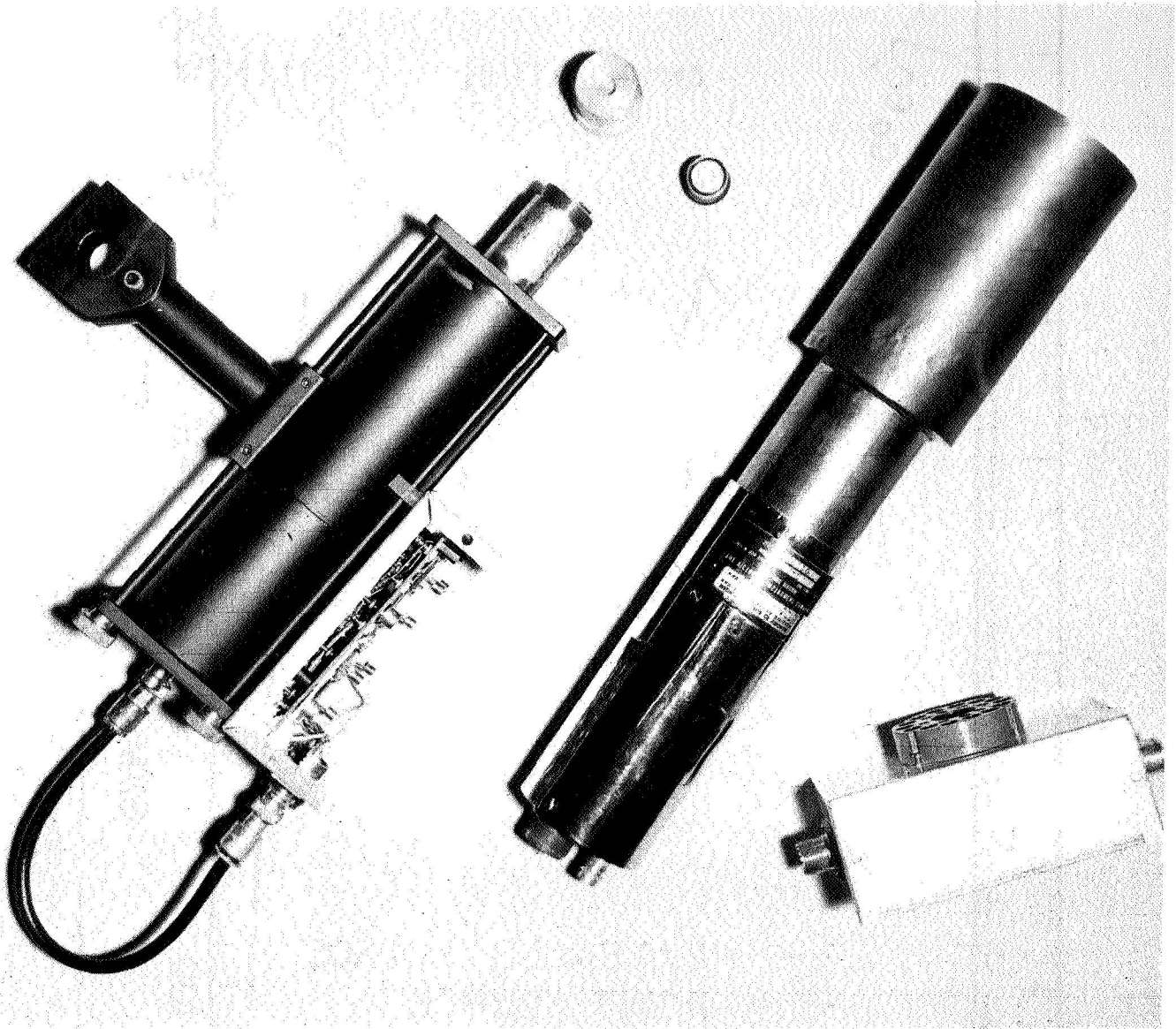
Figure 10.- Scintillation detectors used for phantom exposure measure-
ments. The detector on the left shown with preamplifier case open
can be used with the 1/2-inch-diameter anthracene and 1-inch-diameter
NE 102 thin window phosphors shown at top center which permit admis-
sion of conversion electrons. The 3-inch NE 102 detector (right)
can be used for pulse on total current measurement.
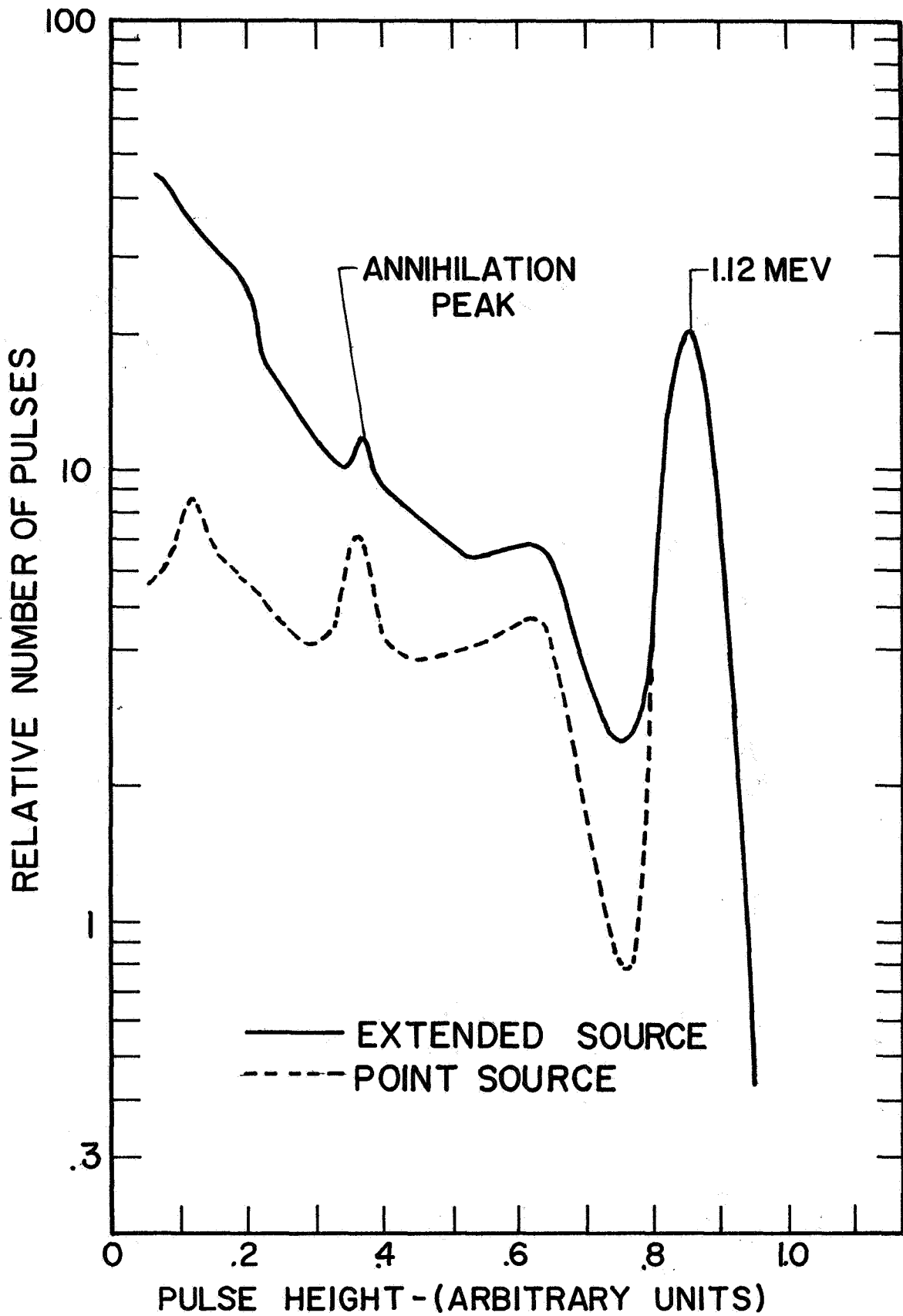
Figure 11.- Comparison of the pulse height spectra of a point and extended gamma source.
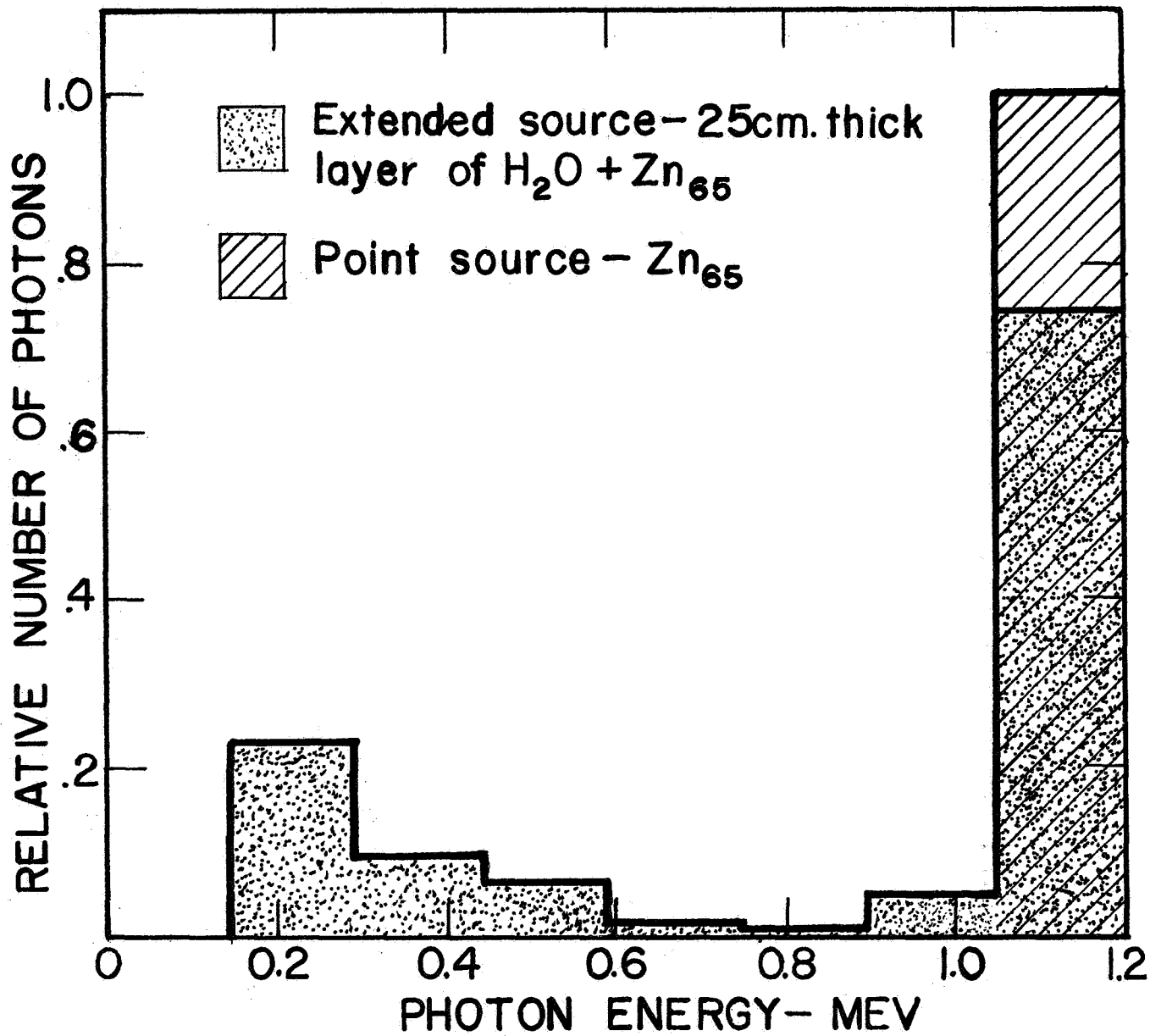
Figure 12.- Histogram of the pulse height spectra of figure 11 after applying an 8 × 8 unscrambling matrix.
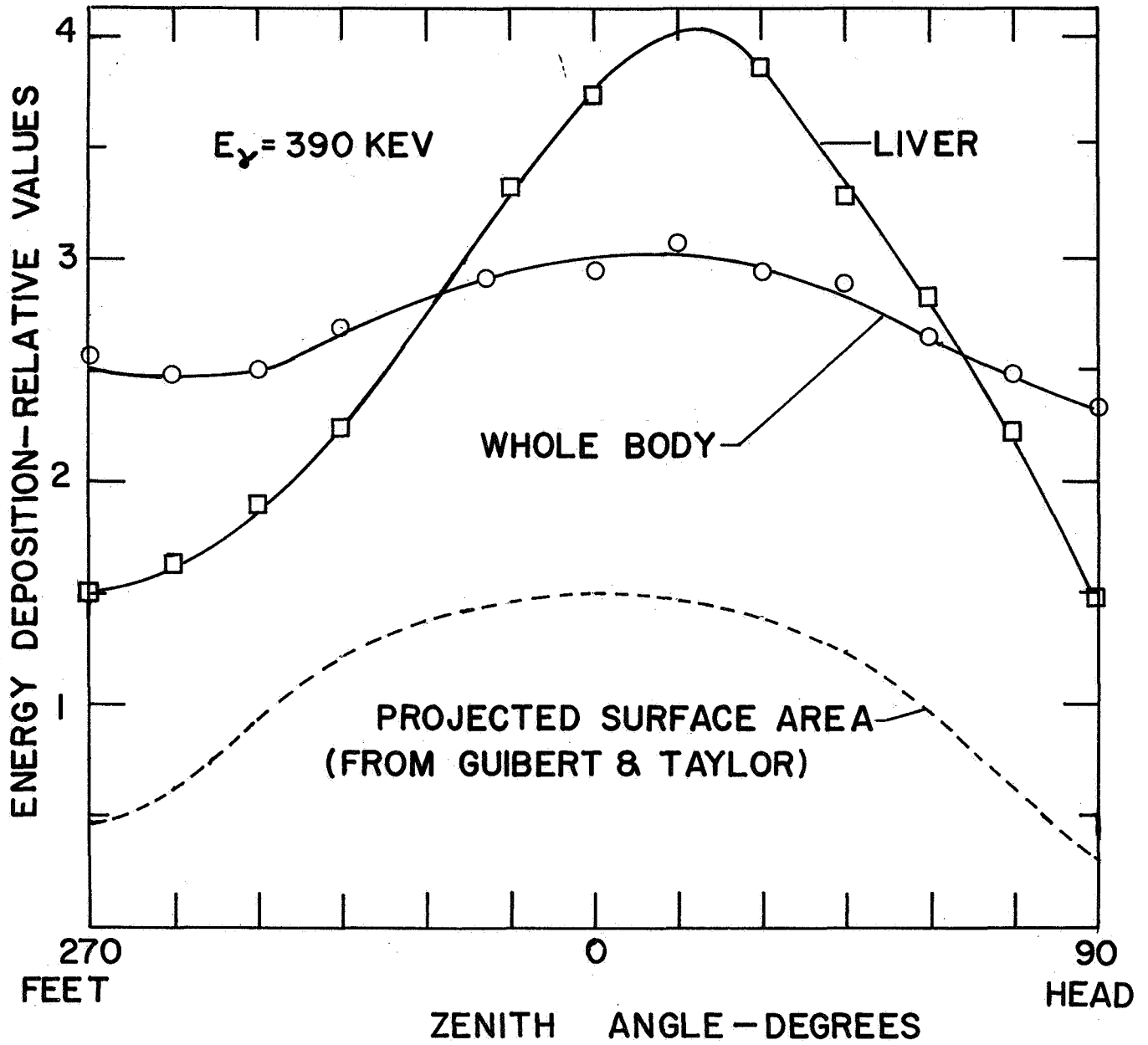
Figure 13.- Variation of average dose with body orientation for
0.39 Mw gamma.